

Superconductivity and fluctuating magnetism in quasi two-dimensional κ -(BEDT-TTF)₂Cu[N(CN)₂]Br probed with implanted muons

T. Lancaster,^{1,*} S.J. Blundell,¹ F.L. Pratt,² and J.A. Schlueter³

¹*Oxford University Department of Physics, Clarendon Laboratory, Parks Road, Oxford, OX1 3PU, UK*

²*ISIS Facility, Rutherford Appleton Laboratory, Chilton, Oxfordshire OX11 0QX, UK*

³*Materials Science Division, Argonne National Laboratory, 9700 South Cass Ave., Argonne, IL 60439, US*

(Dated: July 2, 2010)

A muon-spin relaxation (μ^+ SR) investigation is presented for the molecular superconductor κ -(BEDT-TTF)₂Cu[N(CN)₂]Br. Evidence is found for low-temperature phase-separation, with only a fraction of the sample showing a superconducting signal, even for slow cooling. Rapid cooling reduces the superconducting fraction still further. For the superconducting phase, the in-plane penetration depth is measured to be $\lambda_{\parallel} = 0.47(1) \mu\text{m}$ and evidence is seen for a vortex decoupling transition in applied fields above 40 mT. The magnetic fluctuations in the normal state produce Korringa behavior of the muon spin relaxation rate below 100 K, a precipitous drop in relaxation rate is seen at higher temperatures and an enhanced local spin susceptibility occurs just above T_c .

PACS numbers: 74.70.Kn, 76.75.+i, 74.25.Ha

I. INTRODUCTION

The quasi two-dimensional molecular series κ -(BEDT-TTF)₂X exemplifies the complex interplay of collective phenomena that occur in correlated electron systems^{1,2}. In particular, the proximity of superconducting κ -(BEDT-TTF)₂Cu[N(CN)₂]Br to a Mott transition, along with possible pseudogap physics and molecular disorder effects, has led to this material being extensively studied in recent years³⁻⁷. Despite this intense interest, several experimental observations in this system lack a conclusive explanation² and more experimental study is warranted. In this paper we present a muon-spin relaxation (μ^+ SR) investigation of κ -(BEDT-TTF)₂Cu[N(CN)₂]Br. Our focus is the penetration depth in the vortex state for $T < T_c$ and the fluctuations of the local magnetic field in the normal state.

The layered structure of the κ -(BEDT-TTF)₂X family

of organic molecular metals is shown in Fig. 1(a). The BEDT-TTF molecules dimerize, forming molecular units which stack on a triangular lattice in two-dimensional planes. The removal of one electron from each BEDT-TTF dimer causes the tight-binding band to be half filled and in order to balance the charge layers of anion, X, are located between the partially oxidized BEDT-TTF sheets. The properties of the system are strongly dependent on the transfer integral t which is controlled by the dimer separation and may be manipulated by applying pressure or by changing the identity of the anion². The phase diagram of the family [Fig. 1(b)] shows that the system may be tuned from Mott insulator through superconductivity into a normal metallic state as a function of t/U , where U is the on-site Coulomb repulsion (which is a property of the dimer and is almost independent of the anion or pressure). Importantly, this tuning is achieved without the need for chemical doping (in contrast to the cuprates) and therefore minimizes structural disorder effects. At small t/U Coulomb correlations dominate and κ -(BEDT-TTF)₂X with $X = \text{Cu}[\text{N}(\text{CN})_2]\text{Cl}$ is a Mott insulator⁸. As pressure is increased or X is changed to $X = \text{Cu}[\text{N}(\text{CN})_2]\text{Br}$ there is an insulator-to-superconductor transition⁹. The $X = \text{Cu}(\text{NCS})_2$ compound exhibits a larger t/U still and remains a superconductor with a slightly depressed T_c .

Superconducting κ -(BEDT-TTF)₂Cu[N(CN)₂]Br ($T_c \approx 12$ K) displays several properties [Fig. 2] whose explanation remains obscure. These may be broadly grouped three temperature regions. In region I ($T \approx 80$ K) there are sharp changes in the temperature dependence of the lattice constants⁷ [Fig. 2(d)] and, above 70 K, a rapid increase in the thermal expansion coefficient perpendicular to the planes¹⁰ α_{\perp} [Fig. 2(e)]. These coincide with a rounded maximum in the resistivity¹¹ ρ [Fig. 2(b)]. The properties of this region have been linked to a glass-like freezing of terminal ethylene groups on the BEDT-TTF molecules¹⁰ around $T_g = 77$ K, although it has been suggested⁷ that this

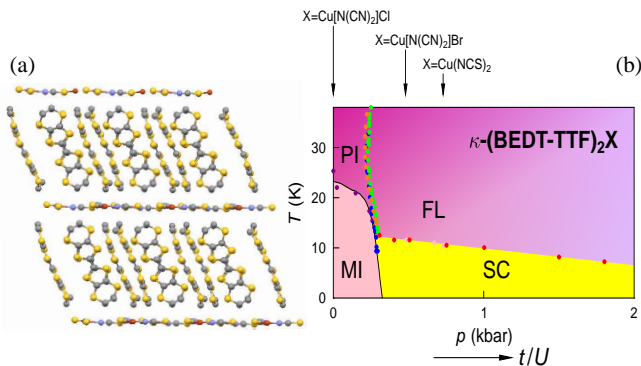


FIG. 1: (a) Layered structure of the κ -(BEDT-TTF)₂X system. (b) Phase diagram of the system showing the proximity of the $X = \text{Cu}[\text{N}(\text{CN})_2]\text{Br}$ salt to the Mott insulator phase. (MI=Mott Insulator, PI=Paramagnetic insulator, SC=Superconductor, FL=Fermi liquid.) (After Ref. 6).

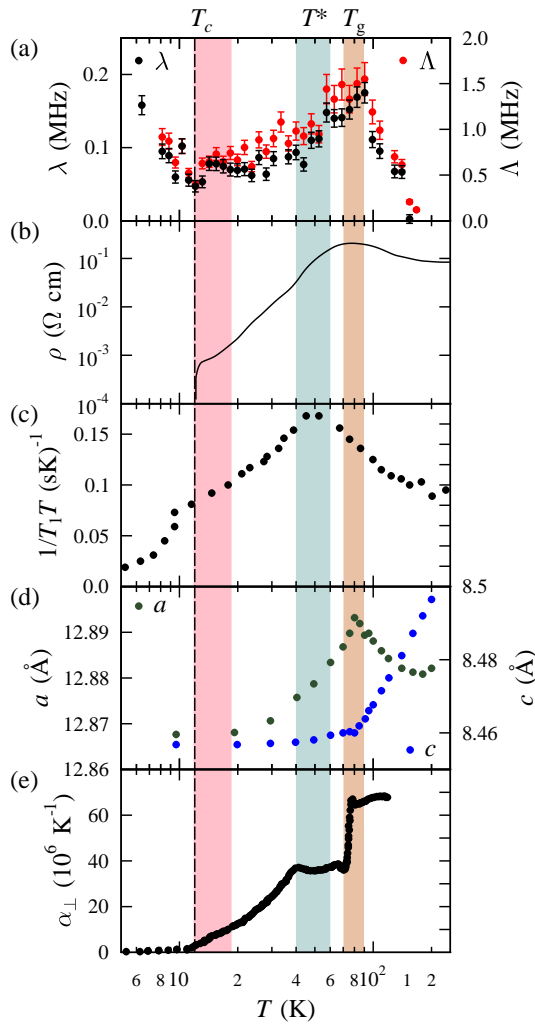


FIG. 2: Comparison of several experimental properties with regions I ($T \approx 80$ K), II ($T \approx 50$ K) and III ($T_c < T \lesssim 18$ K) shaded. (a) LF μ^+ SR relaxation rates (this work); (b) Resistivity¹¹; (c) NMR $1/T_1T$ ¹²; (d) lattice constants⁷; (e) thermal expansion coefficient perpendicular to the layers¹⁰.

freezing alone cannot account for the observed structural changes. In region II ($T \approx 50$ K) NMR measurements^{2,12} yield a maximum in $1/T_1T$ around $T^* \approx 50$ K [Fig. 2(c)]. Upon cooling through this region there is a crossover in transport properties from “bad metal” behavior to a more conventional Fermi-liquid regime² and a plateau in α_\perp is also seen [Fig. 2(e)]. These phenomena have been linked to pseudogap physics although the details remain unclear². In region III ($T_c < T \lesssim 18$ K) a vortex Nernst signal is observed⁶. It was argued⁶ that the proximity of the $X = \text{Cu}[\text{N}(\text{CN})_2]\text{Br}$ material to the Mott state in the phase diagram in Fig. 1(b), results in vortex fluctuations persisting above T_c and, furthermore, this remnant of fluctuating superconductivity may be consistent with the occurrence of phase fluctuations in the superconducting order parameter close to the Mott boundary.

This paper is structured as follows: after discussing experimental details in section II we present the results of transverse field muon-spin relaxation measurements of the superconducting penetration depth of κ -(BEDT-TTF)₂Cu[N(CN)₂]Br in section III. Section IV describes the use of longitudinal field measurements to investigate spin fluctuations in the normal state of the material and our conclusions are presented in section V.

II. EXPERIMENTAL

Muon-spin spectroscopy¹³ is a sensitive means of probing the superconductivity and local magnetism of molecular materials of this sort^{14,15}. Transverse-field (TF) and longitudinal-field (LF) muon-spin relaxation (μ^+ SR) measurements were made on a mosaic sample of κ -(BEDT-TTF)₂Cu[N(CN)₂]Br at the ISIS facility, Rutherford Appleton Laboratory, UK and the Swiss Muon Source (S μ S), Paul Scherrer Institut, CH. The polycrystalline sample was made of ~ 50 small crystallites which grow as platelets whose large faces are parallel to the conducting layers (the ac planes for this material). These were arranged on a piece of Ag foil to cover an area of ≈ 0.5 cm² so that the conducting layers are parallel to the plane of the mosaic. TF measurements were made using the MuSR spectrometer at ISIS where the sample was mounted on a hematite backing plate in a helium cryostat with the sample oriented at 45° to both the applied magnetic field and the initial muon spin. In order to reduce any effect of ethylene disorder on the superconducting properties, the sample was slow cooled at a rate of $\lesssim 5$ K/hour. TF measurements were also made using the GPS instrument at S μ S where the sample plane was oriented at 90° to the applied magnetic field and no slow cooling procedure was followed. LF measurements were made on the ARGUS spectrometer (ISIS) in the latter 90° geometry.

III. TF μ^+ SR AND SUPERCONDUCTIVITY

TF μ^+ SR provides a means of accurately measuring the internal magnetic field distribution in a material, such as that due to the vortex lattice (VL) in a type II superconductor¹⁶. In a TF μ^+ SR experiment spin polarized muons are implanted in the bulk of a material in the presence of a magnetic field $B_{c1} < B_a < B_{c2}$, which is applied perpendicular to the initial muon spin direction. Muons stop at random positions on the length scale of the VL where they precess about the total local magnetic field B at the muon site with frequency $\omega_\mu = \gamma_\mu B$, where $\gamma_\mu = 2\pi \times 135.5$ MHz T⁻¹. The observed property of the experiment is the time evolution of the muon-spin polarization $P_x(t)$, which allows the determination of the distribution $p(B)$ of local magnetic fields across the sample volume via $P_x(t) = \int_0^\infty p(B) \cos(\gamma_\mu Bt + \phi) dB$, where the phase ϕ results from the detector geometry.

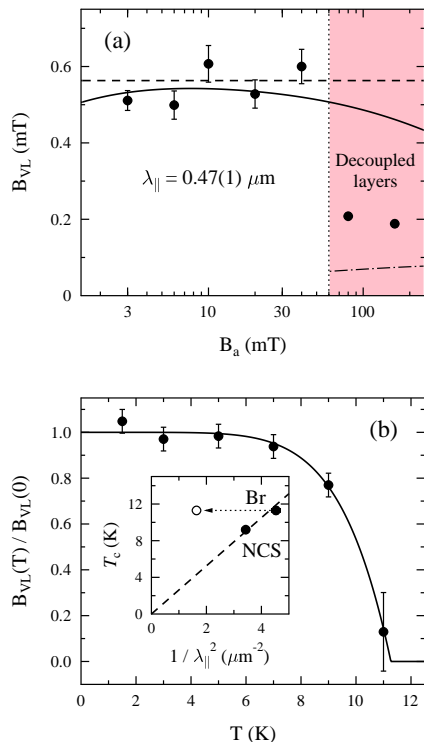


FIG. 3: (a) Broadening of the 1.5 K TF μ^+ SR signal due to the VL measured at $S\mu$ S. The field B_a was applied perpendicular to the conducting layers. The dotted line indicates a transition to a decoupled-layer vortex phase (shaded region) occurring between 40 mT and 80 mT. The solid line is the fit of the field dependent line width¹⁷ below the vortex transition, giving $\lambda_{||} = 0.47(1) \mu\text{m}$; the dashed line is the corresponding width predicted by Eq. (1). The dot-dash line shows the width according to Eq. (2) for fully decoupled vortex layers. (b) Temperature dependence of the normalised VL broadening measured at ISIS in 3 mT field applied at 45° to the sample plane. A fit is shown to Eq. (3). The inset shows scaling^{27,28} between T_c and $\lambda_{||}^{-2}$, comparing the current data (Br) with that of κ -(BEDT-TTF) $_2$ Cu(NCS) $_2$ (NCS)²⁸; the open circle shifted to the left shows the apparent effect of applying $B_a \geq 80$ mT to Br.

Above T_c some broadening of the spectrum is caused by randomly directed nuclear moments relaxing the muon spins. Below T_c the spectrum broadens considerably due to the contribution from the VL, but this component was found to be only $\sim 30\%$ of the total signal for $T < T_c$. Allowing for part of the non-superconducting signal to come from the cryostat and sample mounting material, we estimate that at most 50% of the sample is giving a superconducting signal. This is significant since it suggests that the majority of muons are not stopped in regions where there is a well defined VL and may indicate the coexistence of a competing phase in this material. In fact, there is evidence for a phase separation between superconducting and insulating regions in this material⁴ which is strongly dependent on

disorder, such as that introduced through rapid cooling. The non-superconducting contribution to our signal for $T < T_c$ decreases weakly and linearly with increasing temperature. Rapid cooling of the sample was found to reduce the superconducting volume fraction still further. With such a small superconducting fraction it is difficult to accurately extract detailed lineshape information from our data, however the RMS width of the VL field distribution B_{VL} can be straightforwardly obtained by fitting the data to the sum of two Gaussian relaxation components, reflecting the superconducting VL and non-superconducting contributions. These are easily separated below T_c since the contribution from the VL has a much larger relaxation rate. The field dependence of the VL component is shown in Fig. 3(a). The low field data (40 mT and below) fit well to the width expected from the solution of a Ginzburg-Landau (GL) model of the triangular VL field distribution¹⁷ with an in-plane penetration depth of $0.47(1) \mu\text{m}$. B_{VL} is not very sensitive to B_{c2} in this field range, so we assume the reported value¹⁸ $B_{c2} = 10(2)$ T; the GL parameter κ is then estimated to be $80(10)$. The penetration depth in the highly conducting planes can also be estimated via the approximate expression for a high anisotropy superconductor

$$\lambda_{||} \approx (0.00371)^{\frac{1}{4}} \left[\frac{\Phi_0 \cos \theta}{B_{VL}} \right]^{\frac{1}{2}}, \quad (1)$$

where Φ_0 is the flux quantum and θ is the angle of the applied field with respect to the normal to the plane. This field-independent expression is valid at intermediate fields $B_{c1} \ll B_a \ll B_{c2}$ and the B_{VL} value obtained from Eq. (1) for $\lambda_{||} = 0.47 \mu\text{m}$ is shown as the dashed line in Fig. 3(a); this is seen to be reasonably close to the field-dependent GL width in a field region centred around 10 mT.

Our value of $\lambda_{||}$ is rather smaller than previous reports, e.g. the range $0.57 \leq \lambda_{||} \leq 0.69 \mu\text{m}$ obtained from reversible high field magnetization measurements¹⁹, and it is significantly lower than the value $\lambda_{||} \approx 0.78 \mu\text{m}$ estimated from a previous μ^+ SR measurement²⁰ in a field of 300 mT. These differences can be understood by noting that the measured linewidth decreases sharply for $B_a \geq 80$ mT (Fig. 3(a)). If this suppressed linewidth were taken to represent a full 3D VL, a penetration depth of order $\lambda = 0.80 \mu\text{m}$ would also be obtained from our data using Eq. (1), in good agreement with the previous μ^+ SR result. The decrease in B_{VL} with applied field that we observe is not surprising, given the vortex phase diagram in (BEDT-TTF) $_2$ Cu(SCN) $_2$ ^{14,21}. In that material the ideal 3D triangular VL which exists at low temperatures and low fields²² is destroyed by the application of fields above a disorder-dependent threshold, that can be as low as 6 mT, causing a transition to a decoupled-layer vortex glass phase, accompanied by a sharp decrease in the measured linewidth²¹. It is therefore likely that a similar transition to a decoupled-layer vortex glass phase occurs in the $X = \text{Cu}[\text{N}(\text{CN})_2\text{Br}]$ material above a threshold field in the 40–80 mT region. The effect on the width

TABLE I: Comparison of penetration depth λ_{\parallel} extracted from μ^+ SR measurements under different experimental conditions.

Anion	Study	Skewness	B_a (mT)	λ_{\parallel} (μm)
Cu[N(CN) ₂ Br	This study	0	3-40	0.47(1)
Cu[N(CN) ₂ Br	This study	0.7	3	0.47(1)
Cu[N(CN) ₂ Br	This study	0	160	0.82(1)
Cu[N(CN) ₂ Br	Ref. 20	0	300	0.78
Cu(SCN) ₂	Ref. 14	0.38	2.5	0.54(2)
Cu(SCN) ₂	Ref. 29	0	13-400	0.77(7)

of the field distribution in the limit of losing all inter-layer correlation has been calculated^{23,24}, giving

$$B_{2D}/B_{VL} = 1.4(s/a)^{1/2}, \quad (2)$$

where s is the inter-layer spacing and a is vortex spacing within the layers. This limit is shown as the dot-dash line in Fig. 3(a) and it can be concluded that some residual interlayer correlations remain here since the data points lie significantly above this limit. A further feature of our data in the decoupled vortex phase is that the superconducting fraction recovers to the larger value obtained in measurements made under slow-cooling conditions, suggesting that the disorder-induced phase separation is becoming significantly reduced once the layers are decoupled.

The temperature dependence of B_{VL} has been measured in a field of 3 mT applied in a 45° geometry and this is shown in Fig. 3(b). This can be fitted to an empirical power law

$$B_{VL}(T) = B_{VL}(0)[1 - (T/T_c)^r], \quad (3)$$

where $B_{VL}(0)$ is the zero temperature contribution from the VL. The VL here therefore appears to thermally stable, in contrast to the case of (BEDT-TTF)₂Cu(SCN)₂ where a clear melting of the VL is seen²⁵. The values $B_{VL}(0)=0.31(1)$ mT and $T_c=11.3(4)$ K are obtained from the fit. The penetration depth in the highly conducting planes could be obtained by taking $\theta = 45^\circ$ in Eq. (1), however the absolute accuracy is reduced compared to 90° measurements for two reasons: firstly the width measured at 45° is particularly sensitive to any angular misalignment between the sample and field and secondly the angular scaling in highly anisotropic superconductors can be much more complex than the simple form implied by Eq. (1)²⁶. Returning to the 90° data, we note that a marginally better fit is obtained by allowing for an asymmetric lineshape¹⁴ parameterized using the skewness parameter $\beta = (\langle B \rangle - B_a)/B_{VL}$. The optimum fit is achieved with $\beta = 0.7$, which is reasonably close to the ideal triangular lattice value of 0.60, that was observed in more detailed studies of the vortex phases of the X=Cu(NCS)₂ compound²¹. This fit also yields 0.47(1) μm for λ_{\parallel} . The values obtained here and in previous muon studies for 90° geometry are summarized in Table I. We may compare our values of λ_{\parallel} and T_c for the X=Cu[N(CN)₂]Br material to values obtained previously for the X=Cu(SCN)₂ material. This is shown as

the inset to Fig. 3(b) and suggests that there is a scaling relation between these two parameters. Although this pair of κ -phase points lie rather close, a simple linear scaling²⁷ would be reasonably consistent with the data. More generally, a $T_c \propto \lambda^{-3}$ scaling has been suggested to apply when a broader range of molecular superconductors is considered²⁸, but more data would be required to test whether this holds or not within the subset of κ -phase BEDT-TTF compounds.

IV. LF μ^+ SR AND SPIN FLUCTUATIONS

We now turn to the local magnetic fluctuations in the normal state of this system, which we probe with LF μ^+ SR measurements made in a field of $B = 2$ mT. In these measurements the initial muon spin is directed parallel to the applied field and we measure the polarization $P_z(t)$ along the same direction via the muon asymmetry function $A(t)[\propto P_z(t)]$. Dynamics in the local magnetic field distribution will cause muon spins to flip leading to a depolarization with relaxation rate Λ . The small applied longitudinal field was intended to quench the contribution to the spectra of background from nuclear moments allowing the contribution due to electron spin dynamics to be discerned.

A typical LF μ^+ SR spectrum measured at 20 K is shown in Fig. 4(a). The relaxing amplitude is quite small, but this is not unexpected given previous zero field muon results measured on a related BEDT-TTF material¹⁵. In that study, muons were shown to be sensitive to magnetic order within the organic layers but only a small relaxing asymmetry was observed. We therefore expect that our results will reflect magnetic fluctuations within the organic layers of κ -(BEDT-TTF)₂X. Above 100 K our spectra are best described with a single exponential function with relaxation rate Λ characteristic of dynamic fluctuations in the local magnetic field at the muon sites in the material. For $T < 100$ K, there is a single, highly damped, temperature dependent oscillation visible for times $t \leq 4 \mu\text{s}$. In this context, spectra of this form suggest a contribution from quasistatic disordered magnetic moments which is typically described by a Kubo-Toyabe (KT) function³⁰ $f_{KT}(\Delta, B, t)$ where the data are best fitted with a constant field width $\Delta = 0.72$ MHz for all $T < 100$ K. We note that this is quite large for randomized nuclear fields (where typically $\Delta < 0.3$ MHz)

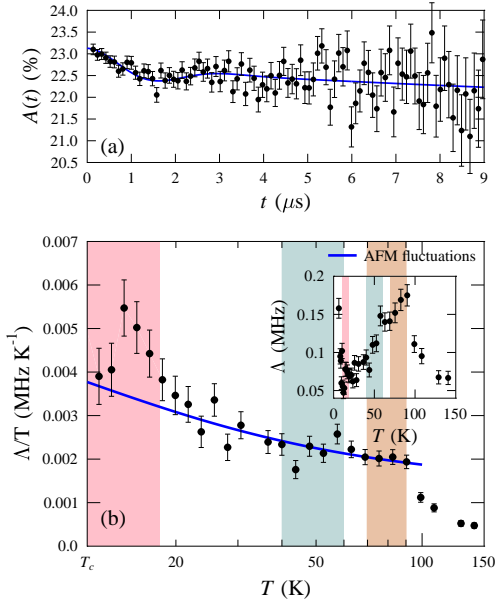


FIG. 4: (a) Typical spectra measured in a LF of $B = 2$ mT at $T = 20$ K. (b) Temperature evolution of Λ/T . Regions I, II and III are shaded and a fit to a model of antiferromagnetic spin fluctuations is shown. Inset: Evolution of Λ with T extracted from fits to Eq. (4).

and given the small size of the electronic moments observed with muons in BEDT-TTF layers previously¹⁵ it may be that this signal results from a population of static disordered electronic moments. The origin of such quasistatic electronic moments is unclear although we note that there is no decrease in Δ with increasing T as would occur in the presence of magnetic order. We note that it is possible that this signal arises from those portions of the sample not contributing to the superconducting VL in TF measurements.

The dynamic contribution to the spectra for $T < 100$ K was found to be best modelled by multiplying the KT function by an exponential factor $e^{-\Lambda t}$ and the data were fitted to the resulting functional form

$$A(t) = A_0 f_{KT}(\Delta, B, t) e^{-\Lambda t} + A_{bg}. \quad (4)$$

The extracted relaxation rates Λ are shown in Fig. 2(a) and inset in Fig. 4(b). Other parameterizations are possible but lead to less successful fits. However, for comparison, a fit across the measured temperature regime of a single exponential with relaxation rate Λ is shown in Fig. 2(a), where we see that both track the same behavior.

At temperatures $T < 100$ K, the dominant trend is a roughly linear increase in relaxation rate with T up to around 100 K, above which it drops precipitously [inset Fig. 4(b)]. The linear regime observed for $T < 100$ K is typical of a Korringa law relaxation³¹, resulting from flip-flop transitions of electronic and muon spins, and which is expected to lead to a relaxation rate $\Lambda = \frac{1}{T_1} \propto$

$k_B T \sum_{\mathbf{q}} A(\mathbf{q})^2 \lim_{\omega \rightarrow 0} \chi''(\mathbf{q}, \omega) / \omega$, where $\chi''(\mathbf{q}, \omega)$ is the imaginary part of the dynamic magnetic susceptibility and $A(\mathbf{q})$ is the hyperfine coupling. For the case of a \mathbf{q} -independent coupling, we obtain $\lambda \propto k_B T [A\chi(0, 0)]^2$, showing that the muon relaxation rate probes the local spin susceptibility $\chi(\mathbf{q} = 0, \omega = 0)$. The sharp decrease in relaxation rate around 100 K broadly coincides with region I, which may suggest a link with the ethylene disorder effects and glass-like transition in this region. Given the Korringa law behavior observed at low temperatures, it is likely that the crossover to nonmetallic behavior of the system near region I [Fig. 2(b)] changes the nature of the muons' coupling to the material and that at these elevated temperatures a different, dominant relaxation channel presumably opens up. To further investigate the temperature evolution of the local susceptibility from the Korringa relaxation we plot $\Lambda/T (\equiv 1/T_1 T)$ against T in Fig. 4(b). We see that on warming above T_c the quantity Λ/T peaks at around 15 K before decreasing sharply around region III ($15 < T \lesssim 25$ K) indicating a significant decrease of the local magnetic susceptibility in this region. Above 30 K Λ/T decreases only gradually throughout region II until dropping off suddenly in region I.

Our muon Λ/T results are quite different to the NMR $1/T_1 T$ results [Fig. 2] where a larger peak is seen in region II. We do not see any dramatic change of behavior in region II in the μ^+ SR results, while there is no suggestion of any anomaly in the NMR behavior in regions I and III. In fact, the NMR results for $50 \text{ K} < T < 300 \text{ K}$ are well described by a model of antiferromagnetic spin fluctuations⁵ based on the MMP model³², which predicts $1/T_1 T \approx A + B/(T/T_x + 1)$, where A and B are constants that depend on the correlation length of the spin fluctuations whose energy scale is determined by the temperature parameter T_x . As shown Fig. 4(b) the model fits the muon Λ only passably well for $T < 100$ K becomes gradually worse as region III approached from above. However, given that the muon sites in this material are likely to be different to the ¹³C site where the nuclear resonance is achieved¹², it is possible that the muon will probe a quite different field distribution to that probed in NMR. We note further that our muon results are also quite different to the LF μ^+ SR behavior observed in molecular superconductors such as the alkali-fullerides³³ where Λ/T is quite featureless above T_c .

V. CONCLUSIONS

In conclusion, our investigation of the superconducting and normal state properties of κ -(BEDT-TTF)₂Cu[N(CN)₂]Br using implanted muons has allowed us to identify a number of experimental features of this system. In the superconducting phase two important effects are seen: firstly, a reduced superconducting signal fraction that is affected by sample cooling rate and is consistent with the phase separation suggested by ear-

lier studies and secondly, a vortex transition taking place between 40 mT and 80 mT, that reduces the width of the magnetic field distribution for higher measurement fields. By taking these two effects carefully into account we have obtained an improved and more reliable estimate for the $T = 0$ in-plane penetration depth $\lambda_{\parallel} = 0.47(1) \mu\text{m}$ and find that the trend of T_c increasing with superfluid stiffness $\rho_s \propto 1/\lambda_{\parallel}^2$ for κ -(BEDT-TTF)₂X superconductors is consistent with the overall trend for molecular superconductors, whereas previous data had suggested that κ -(BEDT-TTF)₂Cu[N(CN)₂]Br was anomalous in this regard. In the normal state we find a large peak in the longitudinal muon spin relaxation rate around 100 K, coinciding with the region where ethylene disorder effects are prevalent. We also observe an enhancement of the local magnetic spin susceptibility above T_c where vortex

fluctuations occur in Nernst measurements. It would be desirable in future to extend μ^+ SR studies of the normal state magnetic properties to the other members of this series in order to follow how these features evolve across the phase diagram.

We are grateful to Alex Amato, Andrew Steele and Peter Baker for experimental assistance and to EPSRC (UK) for financial support. Part of this work was performed at S μ S and part at the STFC ISIS facility and we are grateful to PSI and STFC for the provision of beamtime. Work supported by U. Chicago Argonne, LLC, Operator of Argonne National Laboratory (“Argonne”). Argonne, a U.S. Department of Energy Office of Science laboratory, is operated under Contract No. DE-AC02-06CH11357.

-
- * Electronic address: t.lancaster1@physics.ox.ac.uk
- ¹ T. Ishiguro, K. Yamaji and G. Saito *Organic Superconductors: 2nd edition* (Springer, Berlin) 2006.
 - ² B.J. Powell and R.H. McKenzie, J. Phys.: Condens. Matter **18**, R827 (2006).
 - ³ K. Sano, T. Sasaki, N. Yoneyama and N. Kobayashi, Phys. Rev. Lett. **104**, 217003 (2010).
 - ⁴ O.J. Taylor, A. Carrington and J.A. Schlueter, Phys. Rev. B **77**, 060503(R) (2008).
 - ⁵ E. Yusuf, B.J. Powell, R.H. McKenzie, Phys. Rev. B **75**, 214515 (2007).
 - ⁶ M.-S. Nam, A. Ardavan, S.J. Blundell, J.A. Schlueter, Nature **449**, 584 (2007).
 - ⁷ A.U.B. Wolter, R. Feyerherm, E. Dudzik, S. Söllow, C. Strack, M. Lang and D. Schweitzer, Phys. Rev. B **75**, 104512 (2007).
 - ⁸ F. Kagawa, M. Miyagawa and K. Kanoda, Nature **436**, 534 (2005).
 - ⁹ J.M. Williams *et al.*, Inorg. Chem. **29**, 3272 (1990).
 - ¹⁰ J. Müller, M. Lang, F. Steglich, J.A. Schlueter, A.M. Kini and T. Sasaki, Phys. Rev. B **65**, 144521 (2002).
 - ¹¹ R.C. Yu, J.M. Williams, H.H. Wang, J.E. Thompson, A. M. Kini, K. D. Carlson, J. Ren, M.-H. Whangbo and P.M. Chaikin, Phys. Rev. B **44**, 6932 (1991).
 - ¹² K. Miyagawa, K. Kanoda and A. Kawamoto, Chem. Review, **104**, 5635 (2004).
 - ¹³ S.J. Blundell, Contemp. Phys. **40**, 175 (1999).
 - ¹⁴ S.L. Lee, F.L. Pratt, S.J. Blundell, C.M. Aegerter, P.A. Pattenden, K.H. Chow, E.M. Forgan, T. Sasaki, W. Hayes and H. Keller, Phys. Rev. Lett. **79**, 1563 (1997).
 - ¹⁵ K. Satoh, H. Taniguchi, A. Kawamoto and W. Higemoto, Physica B **374-375**, 99 (2006).
 - ¹⁶ J.E. Sonier, J.H. Brewer, and R.F. Kiefl, Rev. Mod. Phys. **72**, 769 (2000).
 - ¹⁷ E. H. Brandt, Phys. Rev. B **68**, 054506 (2003).
 - ¹⁸ H. Elsinger, J. Wosnitza, S. Wanka, J. Hagel, D. Schweitzer, and W. Strunz, Phys. Rev. Lett. **84**, 6098 (2000).
 - ¹⁹ N. Yoneyama, A. Higashihara, T. Sasaki, T. Nojima and N. Kobayashi, J. Phys. Soc. Jpn. **73**, 1290 (2004).
 - ²⁰ L.P. Le, G.M. Luke, B.J. Sternlieb, W.D. Wu, Y.J. Uemura, J.H. Brewer, T.M. Riseman, C.E. Stronach, G. Saito, H. Yamochi, H.H. Wang, A.M. Kini, K.D. Carlson, J.M. Williams, Phys. Rev. Lett. **68**, 1923 (1992).
 - ²¹ F.L. Pratt, S.L. Lee, C.M. Aegerter, C. Ager, S.H. Lloyd, S.J. Blundell, F.Y. Ogrin, E.M. Forgan, H. Keller, W. Hayes, T. Sasaki, N. Toyota and S. Endo, Synth. Met. **120**, 1015 (2001).
 - ²² L.Ya. Vinnikov, T.L. Barkov, M.V. Kartsovnik and N.D. Kushch, Phys. Rev. B **61**, 14358 (2000).
 - ²³ D.R. Harshman, E.H. Brandt, A.T. Fiory, M. Inui, D.B. Mitzi, L.F. Schneemeyer and J.V. Waszczak Phys. Rev. B **47**, 2905 (1993).
 - ²⁴ E.H. Brandt, Rep. Prog. Phys. **58**, 1465 (1995).
 - ²⁵ F.L. Pratt, S.J. Blundell, T. Lancaster, M.L. Brooks, S.L. Lee, N. Toyota and T. Sasaki, Synth. Met. **152**, 417 (2005).
 - ²⁶ F.L. Pratt, I.M. Marshall, S.J. Blundell, A. Drew, S.L. Lee, F.Y. Ogrin, N. Toyota and I. Watanabe, Physica B, **326**, 374 (2003).
 - ²⁷ Y. J. Uemura *et al*, Phys. Rev. Lett. **62**, 2317 (1989); Y. J. Uemura *et al*, Phys. Rev. Lett. **66**, 2665 (1991).
 - ²⁸ F.L. Pratt and S.J. Blundell, Phys. Rev. Lett. **94**, 097006 (2005).
 - ²⁹ D.R. Harshman, A.T. Fiory, R.C. Haddon, M.L. Kaplan, T. Pfiz, E. Koster, I. Shinkoda and D.Ll. Williams, Phys. Rev. B **49**, 12990 (1994).
 - ³⁰ R.S. Hayano, Y. J. Uemura, J. Imazato, N. Nishida, T. Yamazaki and R. Kubo, Phys. Rev. B **20**, 850 (1979).
 - ³¹ S.J. Blundell and S.F.J. Cox, J. Phys.: Condens. Matter **13**, 2163 (2001).
 - ³² A.J. Millis, H. Monien and D. Pines, Phys. Rev. B **42**, 167 (1990).
 - ³³ W.A. MacFarlane, R.F. Kiefl, S. Dunsiger, J.E. Sonier, J. Chakhalian, J.E. Fischer, T. Yildirim and K.H. Chow, Phys. Rev. B **58**, 1004 (1998).